

Journal of Electronic Imaging

SPIDigitalLibrary.org/jei

Improving a rough set theory-based segmentation approach using adaptable threshold selection and perceptual color spaces

Rocio A. Lizarraga-Morales
Raul E. Sanchez-Yanez
Victor Ayala-Ramirez
Alberto J. Patlan-Rosales



Improving a rough set theory-based segmentation approach using adaptable threshold selection and perceptual color spaces

Rocio A. Lizarraga-Morales, Raul E. Sanchez-Yanez,* Victor Ayala-Ramirez, and Alberto J. Patlan-Rosales

Universidad de Guanajuato DICIS, Department of Electronics Engineering, Carr. Salamanca-Valle de Santiago 3.5+1.8 Km Comunidad de Palo Blanco, 36885 Salamanca Gto., Mexico

Abstract. We propose a color image segmentation approach based on rough set theory elements. Main contributions of the proposed approach are twofold. First, by using an adaptive threshold selection, the approach is automatically adjustable according to the image content. Second, a region-merging process, which takes into account both features and spatial relations of the resulting segments, lets us minimize over-segmentation issues. These two proposals allow our method to overcome some performance issues shown by previous rough set theory-based approaches. In addition, a study to determine the best suited color representation for our segmentation approach is carried out, determining that the best results are obtained using a perceptually uniform color space. A set of qualitative and quantitative tests over a comprehensive image database shows that the proposed method produces high-quality segmentation outcomes, better than those obtained using the previous rough set theory-based and standard segmentation approaches. © The Authors. Published by SPIE under a Creative Commons Attribution 3.0 Unported License. Distribution or reproduction of this work in whole or in part requires full attribution of the original publication, including its DOI. [DOI: [10.1117/1.JEI.23.1.013024](https://doi.org/10.1117/1.JEI.23.1.013024)]

Keywords: color image segmentation; multithreshold segmentation; rough set theory; roughness index; *CIE*Luv.

Paper 13327 received Jun. 14, 2013; revised manuscript received Dec. 6, 2013; accepted for publication Jan. 21, 2014; published online Feb. 18, 2014.

1 Introduction

Color image segmentation has been a central problem in computer vision and pattern recognition systems for many years. Its importance relies on its use as a preanalysis step for images in many applications such as object recognition, tracking, scene understanding, and image retrieval, among others. Segmentation refers to the process of partitioning a digital image into multiple regions that are assumed to correspond to significant objects in the scene. The partition consists of assigning a working label to every pixel within an image, in such a way that pixels with the same label share a set of particular features¹ and, in addition, are spatially connected.

A considerable number of approaches address the problem of color image segmentation, and different authors have focused their efforts to categorize all these techniques. Just to mention a few, we can refer to the surveys by Fu and Mui,² Pal and Pal,³ Cheng et al.,⁴ Lucchese and Mitra⁵ and the most recent work by Vantaram and Saber.⁶ In general, the color image segmentation approaches can be separated into three groups: (1) spatially guided, (2) spatially blind, and (3) miscellaneous,⁶ where the first two categories comprise most of the methods.

On one hand, the main idea of the spatially guided methods is that pixels that are neighbors may have features in common. The goal of such methods is to agglomerate adjacent pixels with, for example, split-and-merge^{7,8} and region-growing^{9,10} strategies. Their main drawback is that, even when the resulting regions in the segmentation are spatially

well connected and compact, there is no guarantee that the segments are homogeneous in a specific feature space. Moreover, sequential design (pixel-by-pixel agglomeration) of these procedures often results in intensive computational schemes with significant memory requirements. Among these approaches, the quality of the segmentation is dependent on the initial seeds selection and homogeneity criteria used. On the other hand, we have the spatially blind algorithms. These methods assume that the color on the surface of an object is unvarying and, therefore, the object will be represented as a cluster of points in a given color space. Because of their simplicity and low computational cost, this kind of method has been widely adopted in the development of segmentation algorithms. Examples of these approaches include clustering^{11–14} and histogram-based approximations.^{15,16} In comparison with the spatially guided techniques, the spatially blind methods present some advantages. For example, comparing with the region-growing approaches, in the spatially blind techniques, there is no need to define the number and placement of the initial seeds. The advantage over the split-and-merge methods is that such methods require a postprocessing refinement in order to accurately capture the shape of the objects.

Among the spatially blind techniques, the histogram-based methods offer some advantages over the clustering approximations. An example of those advantages is that in the histogram-based methods, there is no required *a priori* information about the image like the number of classes or the palette of colors to be used. In the histogram-based techniques, the image histogram is obtained and the representative objects within the scene are identified as significant peaks in the histogram. Depending on the number of peaks, a set of thresholds is established and a multithreshold

*Address all correspondence to: Raul E. Sanchez-Yanez, E-mail: sanchezy@ugto.mx

segmentation is carried out. The disadvantages of this approximation include the sensitivity to noise and intensity variations, the difficulty to identify significant peaks in the histogram, and the fact that the regular histogram ignores the spatial relationship between neighbor pixels.

In order to address the problems of the histogram-based methods, Mohabey and Ray¹⁷ introduced the concept of histon, based on the rough set theory.¹⁸ The histon is an enhancement of the histogram, and it is a representation that associates pixels which are similar in features and may belong to one specific object in the image. The histon has the advantage of associating pixels with similar colors within a spatial neighborhood, resulting in a method which is tolerant to small variations of colors and noises. Additionally, the histon facilitates the selection of significant peaks because they are heightened in comparison with the peaks in a histogram. A further improvement to the histon is the proposal by Mushrif and Ray,¹⁹ where both the histon and the histogram are correlated into a representation named as roughness index. In the Mushrif and Ray method (from now on referred to as RBM, for roughness index-based), the selection of peaks in the roughness index is accomplished by following a succession of fixed criteria, considering a peak as significant if it satisfies a minimum height and distance from other peaks. It deserves attention, in the fact that although those fixed criteria are easy to follow, they might not be appropriate for different distributions where the heights and number of peaks are variable. After the thresholding process in the RBM, a region-merging step is performed in order to avoid over-segmentation. This last step is accomplished only in the feature space, ignoring the spatial relationship between the different regions. Recently, the roughness index-based method has been used for different applications like image retrieval,²⁰ detection of moving objects,²¹ color text segmentation,²² and medical imaging.²³

Concerning the color features representation, it is known that the performance of a color-based segmentation method highly depends on the choice of the color space.²⁴ Different studies have tried to determine the best-suited color representation for a given segmentation approach.^{25–28} Some of them have found that the so-called perceptual color spaces, e.g., *CIE Lab* and *CIE Luv*, are the most appropriate when the resemblance to the human visual system is desirable. The main advantage of these color representations is that the Euclidean distance between two points is approximately proportional to the perceptual difference between the two colors represented by those points. Such a desirable characteristic is not fulfilled by the RGB color space. It is interesting to mention that recently, for the roughness index approximation, there have been studies in alternative color representations like *CIE Luv*²⁹ and HSV.³⁰

Although some problems related with the histogram-based methods have been addressed by the RBM, a number of issues are still observed. Considering those limitations, in this article, we put forward a set of modifications in order to improve the segmentation performance: (1) a different threshold selection method, allowing an automatic adaptation of the peak selection criteria for a given image, (2) an adaptation of a region-merging process, which considers both the features and the spatial relationships among the resulting segments in the image. Furthermore, (3) an analysis and comparison of the use of perceptual color spaces are

conducted in order to determine the more suited color representation for this segmentation approach. Experiments on an extensive database show that these improvements lead to better segmentation results in comparison with the original RBM and other state-of-the-art methods.

This article is organized as follows: in Sec. 2, preliminary concepts of the rough set theory, the histon, and the roughness index are presented. Section 3 describes the modifications and the adaptations carried out to improve the roughness index-based. In Sec. 4, the experiments and results are given, followed by concluding remarks in Sec. 5.

2 Rough Set Theory, the Histon, and the Roughness Index

Rough set theory is one of the most recent approaches for modeling imperfect knowledge. This theory was proposed by Pawlak¹⁸ as an alternative to fuzzy sets and tolerance theory. A rough set is a representation of a vague concept using a pair of precise concepts called lower and upper approximations. The lower approximation is a description of the universe of objects that are known with certainty, whereas the upper approximation is the description of the objects that possibly belong to the set. From this concept of a rough set and in the context of image segmentation with histogram-based methods, Mohabey and Ray¹⁷ have developed the idea of the histon which can be considered as the upper approximation of a rough set.

In order to set the histon definition in the context of a histogram-based segmentation method, let us first define an image $I(m, n, C)$ with $M \times N$ pixels size, where m and n are the image coordinates, $m \in [0, M - 1]$ and $n \in [0, N - 1]$. The parameter $C = \{c_1, c_2, \dots, c_j\}$ denotes the space in which the image is represented, and c_i is the information channel used in such representation. Usually, $j = 3$ for color images, but it may take any positive value. Let us also consider L_i as the maximum number of intensity values in the given channel c_i . Therefore, $I(m, n, c_i) \in [0, L_i - 1]$ is the intensity value for the component c_i of the image at the coordinates (m, n) .

The histogram of an image I is a well-known representation of the frequency distribution of all the intensities that occur in the image. The histogram of a certain color channel i is computed as in Eq. (1)

$$h_i(g) = \sum_{m=0}^{M-1} \sum_{n=0}^{N-1} \delta[I(m, n, c_i) - g], \quad (1)$$

where $\delta(\cdot)$ is the Dirac impulse, and g is a given intensity value $0 \leq g \leq L_i - 1$.

Assuming that the features on the surface of the objects are unvarying, each object in the image may be identified as a peak in the histogram. The association of pixels with intensities related with such peaks leads to the segmentation of the relevant objects in the scene. Unfortunately, such an assumption is not always true and variations in the features on the surface of the objects are commonly found, making the identification of peaks a challenging task. Toward the solution of these uncertainties, the histon is a representation that associates pixels that are similar in features and may belong to one specific object in the image. Additionally, such association is not limited to similarity in features, but also includes the relationship of pixels with their neighbors.

Regarding the histon definition as the upper approximation of a rough set, we consider the similarity between a pixel $I(m, n, c_i)$ and its neighbors within a window W of $P \times Q$ pixels size. The similarity is computed as the Euclidean distance obtained using Eq. (2).

$$d(m, n) = \sum_{p, q \in W} \sqrt{\sum_{c_i \in C} [I(m, n, c_i) - I(p, q, c_i)]^2}. \quad (2)$$

The histon H_i , where i is a given color component in the color space, is computed as in Eq. (3).

$$H_i(g) = \sum_{m=0}^{M-1} \sum_{n=0}^{N-1} [1 + X(m, n)] \delta[I(m, n, c_i) - g], \quad (3)$$

where $\delta(\cdot)$ is the Dirac impulse, g is the intensity value $0 \leq g \leq L - 1$, and $X(\cdot)$ is a matrix which records the pixels that are similar to its neighbors. $X(\cdot)$ is obtained as in Eq. (4).

$$X(m, n) = \begin{cases} 1, & d(m, n) < Ex \\ 0, & \text{otherwise} \end{cases}, \quad (4)$$

where Ex is the distance threshold for a pixel to be considered similar to its neighborhood. In order to process the pixels at the boundaries of the image in the matrix X , pixel values in the edge are mirrored outside the image instead of using zero values. This operation enables us to properly process the whole image under test.

From the above definitions, we can say that the histon, in analogy to the histogram, registers the number of pixels that are similar to its neighbors. For each pixel that is similar in features to its neighbors, the corresponding bin in its intensity channel c_i is incremented twice. This double increment in the histon results in the heightening of peaks, corresponding to locally uniform intensities. The main advantage of using the histon, instead of the regular histogram, is that the histon is able to capture the local similarity, resulting in a representation tolerant to small intensity variations and furthermore, since the peaks are heightened, their detection is easier.

In the rough set theory, the lower and upper sets can be correlated using the concept of roughness index.¹⁹ The roughness index is a representation of the granularity or accuracy of an approximation set. In our scope, the roughness index is the relationship of the histogram and the histon for each intensity level g . The roughness index is defined as in Eq. (5).

$$\rho_i(g) = 1 - \frac{|h_i(g)|}{|H_i(g)|}, \quad (5)$$

where i is the corresponding color component, h is the histogram, H is the histon, and $|\cdot|$ denotes the cardinality in each intensity level g . The value of roughness is close to 1 when

the cardinality of the histon is large in comparison with the cardinality of the histogram in a given intensity value. This situation occurs when there is a high similarity in the features on a given region. If there is a small similarity and high feature variability in the neighborhood, the roughness index tend to be close to 0, because the histon and the histogram have the same, or almost the same, cardinality. In a general sense, the histon and the roughness index give a global distribution of the uniform and connected regions in the image, and each peak represents each one of such regions.

From the roughness index array, a multithresholding method is applied for achieving the final image segmentation. Thresholds in each channel are automatically localized on the valleys between two significant peaks, which represent the meaningful objects in the scene. The final segmentation is the union of the segments for each channel. In this study, we use three color channels; however, it is worth to remark that it is possible to expand this approach for images that have more than three information channels.

3 Improving a Rough Set Theory-Based Segmentation Approach

In this article, we propose to conduct a set of modifications to the RBM.¹⁹ In the RBM method, the selection of thresholds is carried out on the roughness index in each color component of the RGB color space. The criteria used for the selection of the significant peaks and thresholds are based on two nonadjustable rules that were empirically determined. The first one designates a specific height, and the other specifies a minimum distance between two peaks. The height of a significant peak must be above 20% of the average value of the roughness index for all the pixel intensities, and the distance between two potential significant peaks has to be higher than 10 intensity units.

In order to diminish the over-segmentation, the RBM performs a region-merging process where the fusion of two regions takes into account only the color similarity in the feature space, ignoring the spatial relation of the different segments.

The proposed improvements in this article lead to the segmentation approach illustrated in Fig. 1. From now on, this method is referred to as PRM, for perceptual roughness index-based method. In the beginning of the PRM, a color space transformation is applied to the input image, pursuing a representation closer to the human perception. Then, the roughness index computation, a multithresholding method, and an adaptive peak selection are performed. The main improvement in this step is the adaptive peak selection, where the criteria used for choosing the significant peaks change in accordance with the image content. At the end, the segmented image is obtained after a region-merging process, which takes into account both feature similarity and spatial relationships. Each block of Fig. 1 is described in the following subsections.



Fig. 1 The general process of the proposed segmentation approach [perceptual roughness index-based method (PRM)].

3.1 Definition of the Color Spaces Under Analysis and Color Space Transformations

A color space is an abstract representation that describes colors as tuples of numbers, typically as three values or color components.³¹ In the context of image segmentation, it is known that the use of a given color representation has a relevant impact on the performance of a segmentation method.²⁴ Different studies have been oriented to the determination of the best suited color representation for a given segmentation approach^{25–28} and have concluded that the so-called perceptual color spaces provide better results. In this regard, and for our specific method, we explore the use of different color spaces and their impacts in the performance results. We have mainly explored the use of perceptual color spaces *CIELab* and *CIELuv*, because it has been found that they are the most appropriate when the resemblance to the human visual system is desirable. In this section, we describe the required transformations to carry an image from the RGB color space to the perceptual spaces explored in this study.

Given that the perceptual color space transformations are applied to the CIEXYZ space, the transformation of all the images in RGB to the CIEXYZ space must be carried out. The color representation CIE 1931 XYZ, best known as CIEXYZ, is one of the first color spaces obtained from a mathematical model of the human color perception. It was developed by the Commission Internationale de l'Éclairage (CIE) back in 1931.³² The transformation equation is presented in Eq. (6).

$$\begin{bmatrix} X \\ Y \\ Z \end{bmatrix} = \begin{bmatrix} 0.6069 & 0.1735 & 0.2004 \\ 0.2989 & 0.5866 & 0.1145 \\ 0.0000 & 0.0661 & 1.1162 \end{bmatrix} \begin{bmatrix} r \\ g \\ b \end{bmatrix}, \quad (6)$$

where $r, g, b \in [0, 1]$.

The CIE 1976 (L^*, a^*, b^*) color space, better known as *CIELab*, is a space derived from the CIEXYZ color space. The main purpose of its development was to model a perceptually linear space. This means that the Euclidean distance between two points in the space is proportional to the perceptual difference of the colors they represent. The transformation equations to obtain the *Lab* components are defined from Eq. (7)–(10).

$$f(t) = \begin{cases} t^{1/3}, & t > \alpha^3 \\ t/(3\alpha^2) + 16/116 & t \leq \alpha^3 \end{cases} \quad (7)$$

$$L = 116f(Y/Y_n) - 16 \quad (8)$$

$$a = 500[f(X/X_n) - f(Y/Y_n)] \quad (9)$$

$$b = 200[f(Y/Y_n) - f(Z/Z_n)], \quad (10)$$

where $\alpha = 6/29$, and (X_n, Y_n, Z_n) is the reference white for the scene in CIEXYZ. In this work, we have used the standard for a daylight illuminant D65, where $X_n = 95.05$, $Y_n = 100$, and $Z_n = 108.88$.

In the same manner as the *CIELab* color space, the *CIELuv* was developed by the CIE in order to obtain a

perceptually linear space. The transformation equations to take from the CIEXYZ space to the *CIELuv* space are defined in Eqs. (11)–(15).

$$u' = \frac{4X}{X + 15Y + 3Z} \quad (11)$$

$$v' = \frac{9Y}{X + 15Y + 3Z} \quad (12)$$

$$L = 116(Y/Y_n)^{1/3} - 16 \quad (13)$$

$$u = 13L(u' - u'_n) \quad (14)$$

$$v = 13L(v' - v'_n), \quad (15)$$

where Y_n is the Y component of the reference white in CIEXYZ, and u'_n and v'_n are the chromaticity coordinates of the reference white. The inverse transformations of these color spaces are not required because in our study, there is no need to return to the RGB color representation.

In the context of image segmentation, it is known that the use of a given color space has a relevant impact on the general performance. Therefore, the first issue to address in our methodology is to determine the most appropriate color space to be used. Although the RGB space is the most used in the literature, this representation is not useful to mimic the higher level processes that allow the perception of color of the human visual system.⁵ For this reason, we prefer to review the benefits of the representation of the color in terms of a perceptually uniform space. The adaptation of the PRM procedure to use perceptual color spaces is simple. Originally, the RBM approach uses the RGB color space with $L_i = 256$ intensities in each channel i . Once the whole image has been transformed to a given color space, each component is fitted to the range of $[0, 255]$ by adjusting the dynamic range of the image.

3.2 Roughness Index-Based Segmentation

After the transformation and adjustment of the color representation, the second issue to address is the peak/threshold selection procedure for the roughness index in order to perform the multithreshold segmentation. Considering that the selection criteria in RBM are fixed, there is no guarantee that the best peaks are found for all types of images. Therefore, the selection of the thresholds must be adaptive, in such a way that different height and distance criteria are used for different images.

The corresponding block for the roughness index-based segmentation is described in Fig. 2. First, the histogram h_i , the histogram H_i , and the roughness index ρ_i for each color component i are computed. After that, in order to reduce the presence of noise, we filter the roughness index input vector $\rho_i(g)$. Concerning this task, we have tested several linear and nonlinear filters, like averaging filters and rank filters with different window sizes. We have found that the linear filter shown in Eq. (16) offers the best results.

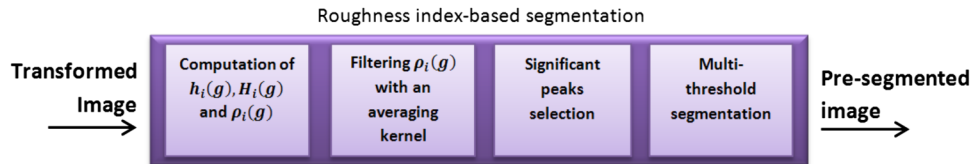


Fig. 2 Internal steps of the roughness index-based method for segmentation.

$$\rho'_i(g) = \frac{\rho_i(g-2) + \rho_i(g-1) + \rho_i(g) + \rho_i(g+1) + \rho_i(g+2)}{5}. \quad (16)$$

After the reduction of possible spurious maxima, we estimate the set of significant peaks adaptively for each image. This is performed by computing the minimum height T_h and the minimum distance T_d between two peaks that have to be attained by a peak to be considered significant.

First, the set of all local maxima $P = \{p_1, p_2, \dots, p_k\}$ is obtained from the filtered roughness index ρ' , where a local maximum p_k is

$$p_k = \{g | \rho'(g) > \rho'(g-1) \wedge \rho'(g) > \rho'(g+1)\}. \quad (17)$$

After we have obtained the k local maxima, we compute the mean μ and the standard deviation σ of their corresponding heights [see Eqs. (18) and (19)].

$$\mu = \frac{1}{k} \sum_{i=0}^k \rho'(p_i), \quad (18)$$

$$\sigma = \sqrt{\frac{1}{k} \sum_{i=0}^k [\rho'(p_i) - \mu]^2}. \quad (19)$$

The same procedure is followed for the distance discrimination. Two peaks that are above the height threshold T_h , which is quantified with $T_h = \mu - \sigma$, must also have a distance to the next peak greater than a distance threshold T_d . In our method, the distance threshold is computed in the same manner as the height threshold T_h . The mean and the standard deviation of the corresponding distances are computed. In the case that two peaks are above T_h but their distance is below T_d , the higher peak is selected as significant. The final

set of threshold values are found on the minimum value between two significant peaks.

3.3 Region Merging

A final point to consider is the region-merging procedure. The region merging is a common tool used to reduce over-segmentation issues. The merging step broadly consists of fusing small regions with neighbor and bigger regions. The fusion criteria may vary from method to method. In the previously proposed RBM, the region merging is carried out following the algorithm by Cheng et al.,¹⁶ where the fusion of two regions takes into account only the color similarity in the feature space, ignoring the spatial relationship of the different segments.

For the region-merging step in our PRM, we take into account both the color similarity and the spatial relationship between regions. The strategy of our method first identifies the small regions whose number of pixels is less than a given threshold. From the experiments, detailed in the next section, we have found that a good minimum number of pixels in a given region to be considered is as small as 0.2% of the whole image size. Once we have identified all the small regions, they are fused with the most appropriate neighbor region. Such a region is one that minimizes the distance between the color components of the segments and maximizes the number of connected pixels between those two regions. Hence, a small region is merged with its neighbor that is more similar in features and has more connected pixels. In case of conflict, the feature similarity is privileged. The process is illustrated in Fig. 3.

4 Experiments and Results

In this section, we present experiments on natural scene images in order to evaluate: (1) the more suited color representation for our segmentation approach, PRM, and (2) the performance of the PRM in comparison with other state-of-the-art approaches. In these experiments, the Berkeley Segmentation Data Set and Benchmarks 500 (BSDS500)⁵³

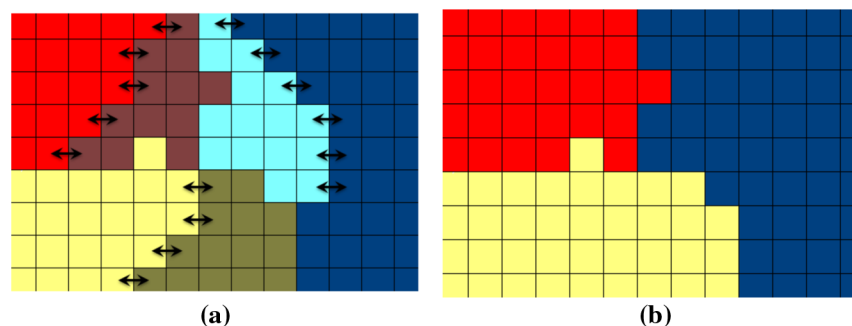


Fig. 3 Initial regions (a) and the final segmentation map after the region-merging process (b) using the two criteria of feature similarity and spatial connectivity.

is used. This dataset is a well-known empirical basis for the evaluation of segmentation algorithms. The advantage of this dataset is that, for each image, a ground truth is available and can be used to quantify the reliability of a given method. Moreover, the diversity of content of this dataset, including landscapes, animals, buildings, and portraits, makes it a challenge for any segmentation algorithm. The BSDS500 is an extension of the Berkeley Segmentation Data Set 300 (BSDS300).³⁴ The BSDS300 consists of 200 training and 100 test images, whereas the BSDS500 proposes the 300 images of BSDS300 for training and adds 200 new images for testing.

For a quantitative evaluation of our segmentation method, three widely used metrics are adopted: the Probabilistic Rand-Index (PRI),³⁵ the Global Consistency Error (GCE),³⁴ and the Boundary Displacement Error (BDE).³⁶ These three metrics evaluate the segmentation result from different perspectives. The BDE measures the average displacement error between the boundary pixels of the segmented image and the closest boundary pixels in the ground-truth segmentations. The GCE evaluates the segments as sets of pixels, and it measures the inconsistencies between the resulting sets in the segmented outcome and in the ground truth. An interesting feature of the GCE is that it is tolerant to refinement in the segmentation. This means that if one segmentation is a subset or a refinement of another segmentation, the GCE value tends to be zero. The PRI counts the number of pairs of pixels whose labels are consistent in both the ground truth and the segmented outcome. This measure is considered the most important in our evaluation because, as pointed out by Yang et al.,³⁷ there is a good correlation between the PRI and the human perception through the hand-labeled segmentations. The PRI measure appears in the range [0, 1], where a resulting value closer to 1 is desirable. For the BDE and GCE, values closer to 0 are better. In order to compute these measures, we have used the MATLAB source code, made publicly available by Yang et al.³⁷

4.1 Performance Evaluation in Different Color Spaces

Before presenting the comparison in different color spaces, let us remark that the rough set-based segmentation methods depend on two parameters (W, Ex), the size of the window W and the expanse Ex , which is the similarity tolerance among colors. Hence, it is important to estimate the best parameters to be used for each evaluated color space and to determine which one is the best representation for our approach.

In the RBM that uses the RGB color space, the best couple of parameters proposed by the authors is (3, 100). In contrast, as the perceptual color spaces have different shapes in comparison with the RGB color space, we must estimate the more suitable parameters for them. The evaluation of the best combination of parameters is carried out using the 300 training images taken from the BSDS500 and are quantitatively assessed with the PRI, BDE, and GCE measures. We have exhaustively searched for the best window size W in the set {3, 5, 7, 9, 11} and the expanse Ex in the set {50, 100, 150, ..., 400}. We have found that the best parameters for the RGB space using our method are (5, 150). In the case of the CIE_{Lab} space, the best set is (7, 150). Using the CIE_{Luv} color space, the best parameters found are (5, 300).

Table 1 Average performance and comparison in three color spaces using the 300 training images in the BSDS500.

	PRM _{RGB}	PRM _{Luv}	PRM _{Lab}
PRI	0.737	0.752	0.760
Standard deviation PRI	0.133	0.133	0.126
PRI > 0.7 (# images)	210	219	226
GCE	0.245	0.203	0.213
BDE	11.74	11.42	11.59

Note: The best performance for each measure is shown in bold.

The quantitative comparison of the use of different color representations in the PRM was carried out. The corresponding PRM_{RGB}, PRM_{Lab}, and PRM_{Luv} are implementations of our PRM in RGB, CIE_{Lab} , and CIE_{Luv} color spaces, respectively. Each implementation uses the best parameter set for the corresponding color space. The average PRI, GCE, and BDE results for each color space with the 300 training images are detailed in Table 1, where the best result for each measure is highlighted with bold typeface. In this table, the higher PRI average is achieved by PRM_{Lab} with a value of 0.760. The use of the CIE_{Luv} space is slightly behind 0.752, and the lower average value is achieved by the PRM in RGB with a value of 0.737. In Table 1, the standard deviation and the number of images with a PRI value higher than 0.7 are also presented. The value of 0.7 is taken, because it is empirically considered that images that obtain that PRI value, or above it, are good segmentations. In the same manner, the best results are obtained with the PRM_{Lab}, with the lowest standard deviation and the higher number of images with PRI scores above 0.7. For the GCE and BDE averages, the best results are achieved by PRM_{Luv} with 0.203 and 11.42, respectively. The PRM_{Lab} is slightly behind with 0.212 and 11.59 in average, for the same error measures.

In order to explore the impact on the performance with a different set of images than the training set and to compare

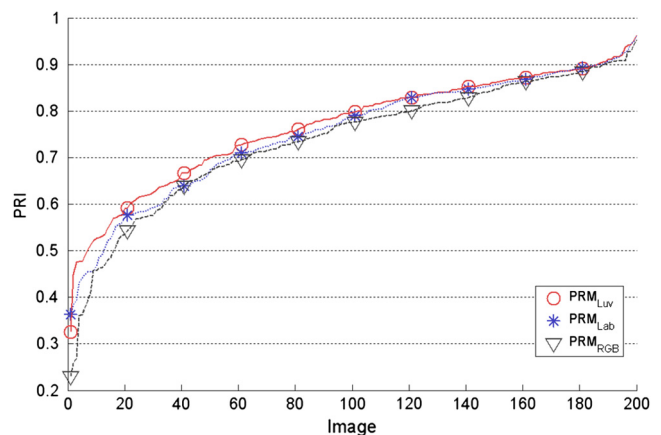


Fig. 4 Comparison of the Probabilistic Rand-Index (PRI) results of our approach in the three color spaces RGB, CIE_{Lab} , and CIE_{Luv} . A higher PRI value is desirable.

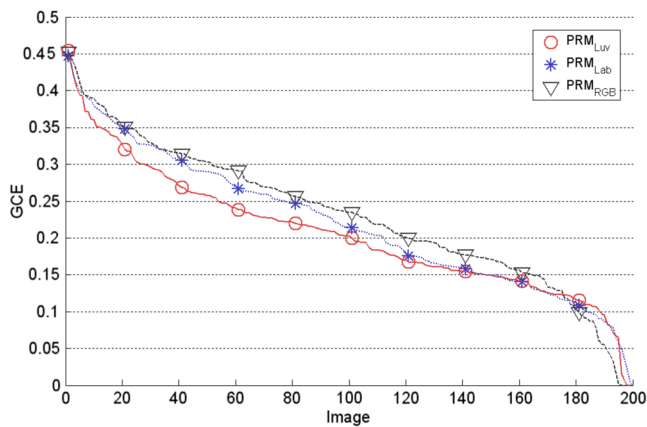


Fig. 5 Comparison of the Global Consistency Error (GCE) results of our approach in the three color spaces RGB, *CIELab*, and *CIEluv*. A low GCE value is desirable.

the results, we have tested the PRM on the 200 test images in the BSDS500. In Figs. 4, 5, and 6, the plots corresponding to the PRI, GCE, and BDE measures are provided for each test image. The PRI values are plotted in increasing order, whereas for the GCE and BDE, the values are plotted in decreasing order. Hence, a given index in the horizontal axis may not represent the same image across the algorithms. In this way, we can evaluate the quality tendencies of each method and compare them. As we can see from these figures, the curves related to the use of perceptual color spaces are consistently better than the curve representing the RGB space. However, it is observed that both PRM_{Lab} and PRM_{Luv} curves are very close and from a visual inspection, it is hard to determine which space is the most appropriate for our method. In this case, the quantitative results enable us to do a much clearer distinction between the performance of PRM_{Lab} and PRM_{Luv} . The corresponding average results for the 200 test images are detailed in Table 2. It is likely to be noticed that the best performance for each quantitative measure is achieved by the PRM_{Luv} , which means that the use of *CIEluv* color space in our method is the most suitable and provides more stability. The PRI value is 0.768 with a low standard deviation of 0.120, and 150 images with a PRI result above 0.7. In relation with the error measures

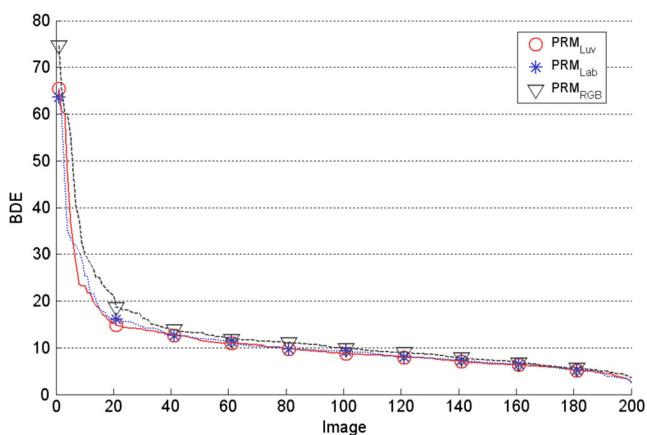


Fig. 6 Comparison of the Boundary Displacement Error (BDE) results of our approach in the three color spaces RGB, *CIELab*, and *CIEluv*. A low BDE value is desirable.

Table 2 Average performance and comparison in three color spaces using the 200 test images in the BSDS500.

	PRM_{RGB}	PRM_{Luv}	PRM_{Lab}
PRI	0.738	0.768	0.754
Standard deviation PRI	0.142	0.120	0.132
PRI > 0.7 (# images)	137	150	143
GCE	0.229	0.205	0.219
BDE	12.50	10.72	10.87

Note: The best performance for each measure is shown in bold.

GCE and BDE, the PRM_{Luv} is the one that attains the minimum error values.

Qualitative examples of the segmentation results using PRM are shown in Fig. 7. In each row, the original image and the corresponding outcome for each color space are visually compared. The original image is shown in the first row, while the resultant segmentation of the PRM using the RGB space is shown in the second row. The corresponding segmentations of the PRM_{Luv} and PRM_{Lab} are shown in the third and fourth rows, respectively. From this qualitative comparison, we can observe that the resulting segmentations of the perceptual spaces outperform the results using the RGB color representation. It can be seen that, in these examples, the outputs from the PRM_{RGB} show a clear over-segmentation, and the PRM_{Luv} and PRM_{Lab} succeed in associating regions with similar colors.

4.2 Performance Comparison with Other Methods

After the study of the PRM in different color spaces, a comparison of our approach in the *CIEluv* color space PRM_{Luv} against other rough set theory-based segmentation methods is conducted. The comparison is carried out with the roughness index-based technique (RBM)¹⁹ and the roughness approach through smoothing local difference (referred to as RSLD).²⁹ The RSLD method is of special interest, since it is a roughness index-based performed on the perceptual color space *CIEluv*. The results for the normalized cuts method (NCuts)³⁸ and the mean shift segmentation approach¹¹ are also included. The NCuts and mean shift methods are considered in this comparison because of their influence as widely used methods in image segmentation tasks. Besides, they are considered as *de facto* standard references for evaluation purposes. It is important to mention that the outcomes of the RBM and the RSLD methods were obtained with our implementation of the algorithms described by the authors. The outcomes from the NCuts and mean shift methods were obtained with publicly available code.

The average PRI, GCE, and BDE results for all methods, using the 300 images for training from BSDS500, are displayed in Table 3. From this table, we can see that the higher average value of 0.752 is achieved by PRM_{Luv} , followed by the RBM with an average of 0.743. The lowest $PRI_{average}$ is obtained with the RSLD method with 0.620. In this table, again, our method obtains more images with PRI values

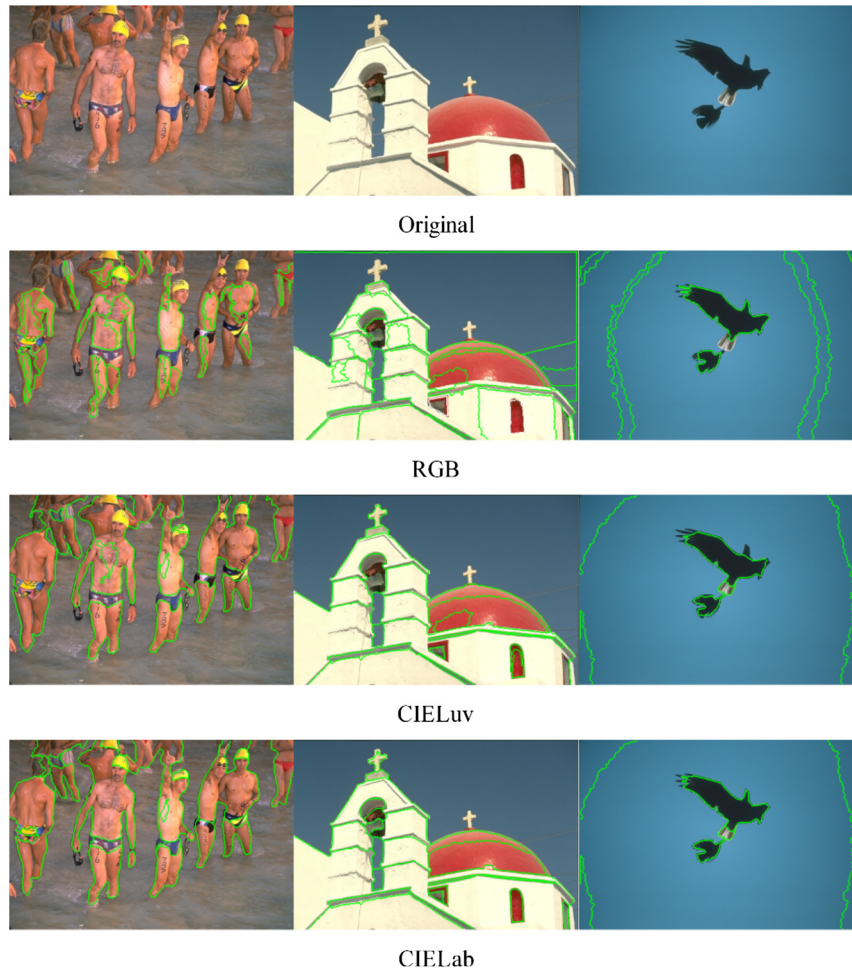


Fig. 7 Qualitative comparison of three samples (first row) out of 500 images from the BSDS500 in the different color spaces under analysis (RGB in the second row and *CIELuv* and *CIELab* on the third and fourth rows, respectively).

higher than 0.7. In this case, the approximation with the lowest standard deviation is the NCuts method with 0.119. However, our approximation is the second more precise method with a standard deviation of 0.133. In the case of GCE and BDE measures, the minor error values are attained by the PRM_{Luv} .

The corresponding results for the 200 test images in the BSDS500 were also obtained and compared. In Figs. 8, 9, and 10, the PRI, GCE, and BDE values, respectively, are

Table 3 Average performance and comparison with other methods using the 300 training images in the BSDS500.

	PRM_{Luv}	RBM	RSLD	Mean shift	NCuts
PRI	0.752	0.743	0.620	0.653	0.722
Standard deviation PRI	0.133	0.135	0.176	0.204	0.119
PRI > 0.7 (# images)	219	180	114	141	200
GCE	0.203	0.302	0.230	0.270	0.298
BDE	11.42	15.75	15.18	11.98	14.05

Note: The best performance for each measure is shown in bold.

plotted. We can observe from Fig. 8 that the PRM_{Luv} and mean shift corresponding results are very close on the top of the curves. It is interesting to notice that the NCuts curve in this figure records higher PRI values than the mean shift, RBM, and RSLD methods for the first 40 images and keeps its superiority over the RSLD method until image

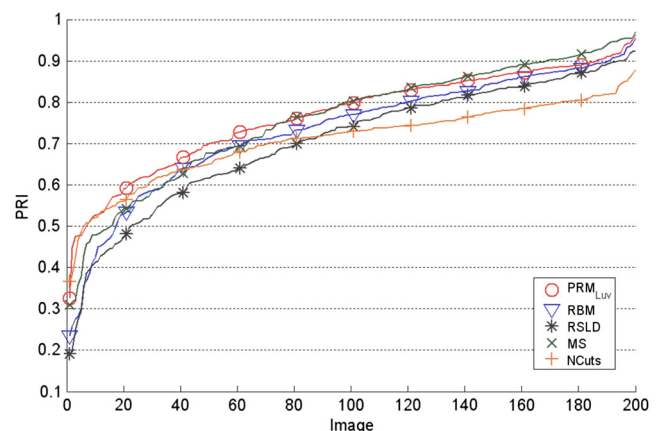


Fig. 8 Comparison of the PRI results of our method PRM_{Luv} with other rough set-based methods (RBM and RSLD) and reference methods (NCuts and mean shift) using the 200 test images from the BSDS500. A high PRI value is desirable.

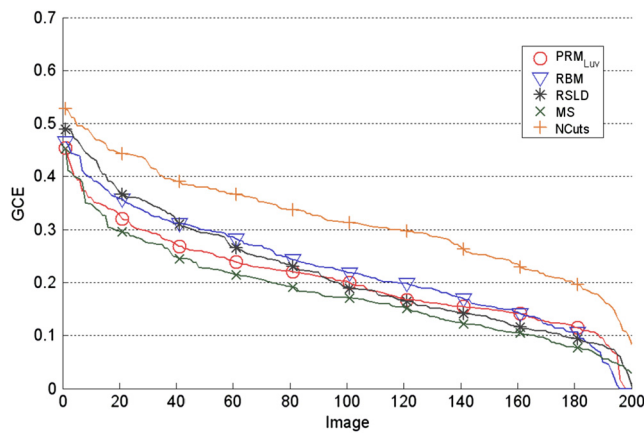


Fig. 9 Comparison of the GCE results of the PRM_{Luv} with RBM and RSLD and the reference methods NCuts and mean shift using the 200 test images from the BSDS500. A low GCE value is desirable.

90. Nevertheless, since the NCuts corresponding curve grows slowly, it drops below the rest of the algorithms from there on. The reason of this trend is that most of the resultant segmentations using NCuts attain a PRI value lower than 0.8 and that they tend to be very close to the mean of 0.722.

In the case of Fig. 9, the curve with the lowest values is the one representing the mean shift approach and the curve with the highest errors is the NCuts one. It is difficult to make a visual separation of methods in Fig. 10, since the PRM_{Luv} , RBM, RSLD, and mean shift curves are very close. The corresponding curve of the NCuts for the BDE measure is the only one that stands out from the rest of the curves, having the highest error values.

The averages of the quantitative measures for each method using the specific test set of images from the BSDS500 are shown in Table 4. For this set of 200 images, the higher PRI is achieved by the PRM_{Luv} with an average of 0.768, a standard deviation of 0.120, and 150 of the 200 images with a PRI value higher than 0.7. The second best is the mean shift method with a PRI average of 0.759 with a standard deviation of 0.148 and 137 images with a PRI value above 0.7. The lowest errors measured with the GCE and

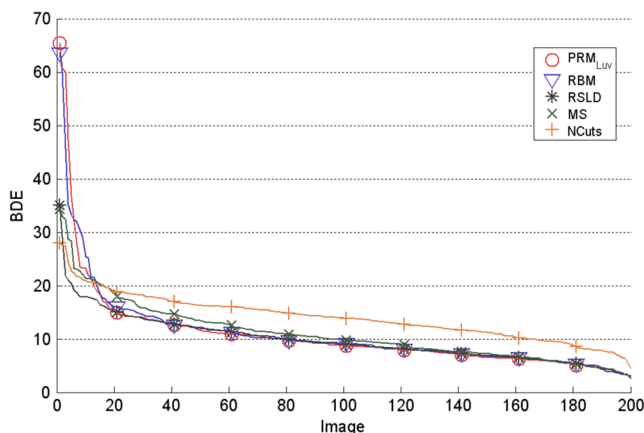


Fig. 10 Comparison of the BDE results of the PRM_{Luv} with RBM and RSLD and the reference methods NCuts and mean shift using the 200 test images from the BSDS500. A low BDE value is desirable.

Table 4 Average performance and comparison with other methods using the 200 test images in the BSDS500.

	PRM_{Luv}	RBM	RSLD	Mean shift	NCuts
PRI	0.768	0.734	0.707	0.759	0.708
Standard deviation PRI	0.120	0.147	0.154	0.148	0.098
PRI > 0.7 (# images)	150	138	117	137	137
GCE	0.205	0.224	0.217	0.180	0.317
BDE	10.72	12.61	13.88	11.02	14.01

Note: The best performance for each measure is shown in bold.

BDE are reached by the mean shift with 0.18 and the PRM_{Luv} with 10.72, respectively. In both cases, the largest errors are obtained by the NCuts. These errors occur because in the original method, the color image is processed using only the lightness component, hence ignoring the chromatic information.

These results of the PRM_{Luv} indicates that this method has the best segmentation performance with high consistency and low error. In general, it is observed that the use of the proposed significant peaks selection, jointly with the merging strategy and the use of perceptual color spaces, improves the segmentation results with respect to the original proposal RBM. Moreover, the presented modifications allow better results in comparison with other classic segmentation methods in terms of the PRI measure.

5 Conclusion

In this article, a set of modifications was proposed in order to improve a rough set theory-based segmentation method. This methodology takes advantage of the integration of spatial information about the pixels and the association of similar colors. The spatial information is added in two places: (1) within the histogram representation, through the similarity computation of neighbor pixels, and (2) in the region-merging process, in which not only the similarity in the feature space is taken into account, but also the connectivity between two segments is considered. The proposed improvements are basically three. First, the use of perceptually uniform color spaces instead of the RGB color representation. From a quantitative evaluation, we have found that the $CIELuv$ color space is the most suited representation for our specific segmentation method; meanwhile the $CIELab$ space has a performance only slightly inferior. The use of a perceptual color representation allows our system to improve performance in the association of similar colors. The second improvement is an adaptive selection of the most suitable thresholds for a given image. The third one is the use of a region-merging process, which includes constraints about both spatial relation and color similarity, reducing over-segmentation problems. Experiments on an extensive database show that these modifications result in a method with better outcomes, outperforming other rough set theory-based approaches and classic reference segmentation algorithms.

Acknowledgments

R. A. Lizarraga-Morales and A. J. Patlan-Rosales acknowledge the Mexican National Council of Science and Technology (CONACyT) for the grant provided.

References

- L. Shapiro and G. Stockman, *Computer Vision*, Prentice-Hall, Upper Saddle River, New Jersey (2001).
- K.-S. Fu and J. K. Mui, "A survey on image segmentation," *Pattern Recognit.* **13**(1), 3–16 (1981).
- N. R. Pal and S. K. Pal, "A review on image segmentation techniques," *Pattern Recognit.* **26**(9), 1277–1294 (1993).
- H. Cheng et al., "Color image segmentation: advances and prospects," *Pattern Recognit.* **34**(12), 2259–2281 (2001).
- L. Lucchese and S. Mitra, "Color image segmentation: a state-of-the-art survey," *Proc. Indian Natl. Sci. Acad.* **67**(2), 207–221 (2001).
- S. R. Vantaram and E. Saber, "Survey of contemporary trends in color image segmentation," *J. Electron. Imaging* **21**(4), 040901 (2012).
- X. Wu, "Adaptive split-and-merge segmentation based on piecewise least-square approximation," *IEEE Trans. Pattern Anal. Mach. Intell.* **15**(8), 808–815 (1993).
- T. Ojala and M. Pietikäinen, "Unsupervised texture segmentation using feature distributions," *Pattern Recognit.* **32**(3), 477–486 (1999).
- J. Fan et al., "Automatic image segmentation by integrating color-edge extraction and seeded region growing," *IEEE Trans. Image Process.* **10**(10), 1454–1466 (2001).
- S. Y. Wan and W. E. Higgins, "Symmetric region growing," *IEEE Trans. Image Process.* **12**(9), 1007–1015 (2003).
- D. Comaniciu and P. Meer, "Mean shift: a robust approach toward feature space analysis," *IEEE Trans. Pattern Anal. Mach. Intell.* **24**(5), 603–619 (2002).
- T. Kanungo et al., "An efficient k-means clustering algorithm: analysis and implementation," *IEEE Trans. Pattern Anal. Mach. Intell.* **24**(7), 881–892 (2002).
- M. Mignotte, "Segmentation by fusion of histogram-based k-means clusters in different color spaces," *IEEE Trans. Image Process.* **17**(5), 780–787 (2008).
- Y. S. Chen, B. T. Chen, and W. H. Hsu, "Efficient fuzzy c-means clustering for image data," *J. Electron. Imaging* **14**(1), 013017 (2005).
- F. Kurugollu, B. Sankur, and A. Harmanci, "Color image segmentation using histogram multithresholding and fusion," *Image Vision Comput.* **19**(13), 915–928 (2001).
- H. Cheng, X. Jiang, and J. Wang, "Color image segmentation based on homogram thresholding and region merging," *Pattern Recognit.* **35**(2), 373–393 (2002).
- A. Mohabey and A. Ray, "Rough set theory based segmentation of color images," in *Fuzzy Information Processing Society, 2000. NAFIPS. 19th Int. Conf. of the North American*, pp. 338–342, IEEE, New York, NY (2000).
- Z. Pawlak, "Rough sets," *Int. J. Comput. Inf. Sci.* **11**(5), 341–356 (1982).
- M. M. Mushrif and A. K. Ray, "Color image segmentation: rough-set theoretic approach," *Pattern Recognit. Lett.* **29**(4), 483–493 (2008).
- N. I. Ghali, W. G. Abd-Elmonim, and A. E. Hassanien, "Object-based image retrieval system using rough set approach," *Adv. Reasoning Based Image Process. Intell. Syst.* **29**, 315–329 (2012).
- P. Chiranjeevi and S. Sengupta, "Robust detection of moving objects in video sequences through rough set theory framework," *Image Vision Comput.* **30**(11), 829–842 (2012).
- S.-J. Hu and Z.-G. Shi, "A new approach for color text segmentation based on rough set theory," in *Proc. 3rd Int. Conf. Teaching and Computational Science (WTCS 2009)*, Vol. 116, pp. 281–289, Springer, Berlin, Heidelberg (2012).
- A. E. Hassanien et al., "Rough sets and near sets in medical imaging: a review," *IEEE Trans. Inf. Technol. Biomed.* **13**(6), 955–968 (2009).
- L. Busin et al., "Color space selection for color image segmentation by spectral clustering," in *2009 IEEE Int. Conf. Signal and Image Processing Applications*, pp. 262–267, IEEE, New York, NY (2009).
- P. Guo and M. Lyu, "A study on color space selection for determining image segmentation region number," in *Proc. Int. Conf. Artificial Intelligence*, Vol. 3, pp. 1127–1132, CSREA Press, Las Vegas, NV (2000).
- L. Busin, N. Vandenbroucke, and L. Macaire, "Color spaces and image segmentation," *Adv. Imaging Electron Phys.* **151**(7), 65–168 (2008).
- F. Correa-Tome, R. Sanchez-Yanez, and V. Ayala-Ramirez, "Comparison of perceptual color spaces for natural image segmentation tasks," *Opt. Eng.* **50**(11), 117203 (2011).
- L. Shafarenko, H. Petrou, and J. Kittler, "Histogram-based segmentation in a perceptually uniform color space," *IEEE Trans. Image Process.* **7**(9), 1354–1358 (1998).
- X. Yue et al., "Roughness approach to color image segmentation through smoothing local difference," in *Rough Sets and Knowledge Technology, Lecture Notes in Computer Science*, J. T. Yao et al., Eds., Vol. 6954, pp. 434–439, Springer, Berlin, Heidelberg (2011).
- A. Ferone, S. Pal, and A. Petrosino, "A rough-fuzzy HSV color histogram for image segmentation," in *Image Analysis and Processing ICIAP 2011, Lecture Notes in Computer Science*, G. Maino and G. L. Foresti, Eds., Vol. 6978, pp. 29–37, Springer, Berlin, Heidelberg (2011).
- M. Fairchild, *Color Appearance Models*, 2nd ed., Wiley, Hoboken, New Jersey (2005).
- T. Smith and J. Guild, "The C.I.E. colorimetric standards and their use," *Trans. Opt. Soc.* **33**(3), 73–134 (1932).
- P. Arbelaez et al., "Contour detection and hierarchical image segmentation," *IEEE Trans. Pattern Anal. Mach. Intell.* **33**(5), 898–916 (2011).
- D. Martin et al., "A database of human segmented natural images and its application to evaluating segmentation algorithms and measuring ecological statistics," in *Proc. 8th Int. Conf. Computer Vision*, Vol. 2, pp. 416–423, IEEE, New York, NY (2001).
- R. Unnikrishnan, C. Pantofaru, and M. Hebert, "A measure for objective evaluation of image segmentation algorithms," in *Proc. IEEE Conf. Computer Vision and Pattern Recognition*, Vol. 3, pp. 34–41, IEEE, New York, NY (2005).
- J. Freixenet et al., "Yet another survey on image segmentation: region and boundary information integration," in *Computer Vision ECCV 2002, Lecture Notes in Computer Science*, Vol. 2352, A. Heyden, G. Sparr, M. Nielsen, and P. Johansen, Eds., pp. 408–422, Springer, Berlin, Heidelberg (2002).
- A. Y. Yang et al., "Unsupervised segmentation of natural images via lossy data compression," *Comput. Vision Image Understanding* **110**(2), 212–225 (2008).
- J. Shi and J. Malik, "Normalized cuts and image segmentation," *IEEE Trans. Pattern Anal. Mach. Intell.* **22**(8), 888–905 (2000).

Rocio A. Lizarraga-Morales received the BEng degree in electronics in 2005 from the Instituto Tecnológico de Mazatlán and the MEng degree in electrical engineering in 2009 from the Universidad de Guanajuato, Mexico. She is currently working toward her DEng degree also at the Universidad de Guanajuato. Her current research interests include image and signal processing, pattern recognition, and computer vision.

Raul E. Sanchez-Yanez concluded his studies of Doctor of Science (optics) at the Centro de Investigaciones en Óptica (Leon, Mexico) in 2002. He also has a MEng degree in electrical engineering and a BEng in electronics, both from the Universidad de Guanajuato, where he has been a tenure track professor since 2003. His main research interests include color and texture analysis for computer vision tasks and the computational intelligence applications in feature extraction and decision making.

Victor Ayala-Ramirez received his BEng in electronics and the MEng in electrical engineering from the Universidad de Guanajuato in 1989 and 1994, respectively, and the PhD degree on industrial computer science from Université PaulSabatier (Toulouse, France) in 2000. He has been a tenure track professor at the Universidad de Guanajuato, Mexico, since 1993. His main research interest is the design and development of soft computing techniques for applications in computer vision and mobile robotics.

Alberto J. Patlan-Rosales received his BEng in computer systems in 2012 from the Universidad de Guanajuato, Mexico. His current research interests include image processing, computer vision, pattern recognition, and rough sets.